Characterisation of the gene family encoding acetoacetyl-CoA thiolase in *Arabidopsis*

Iván Ahumada[A,C], *Albert Cairó*[A], *Andréa Hemmerlin*[B], *Víctor González*[A,D], *Irene Pateraki*[A], *Thomas J. Bach*[B], *Manuel Rodríguez-Concepción*[A,D], *Narciso Campos*[A] *and Albert Boronat*[A,E]

[A]Departament de Bioquímica i Biologia Molecular, Facultat de Biologia, Universitat de Barcelona, Avda. Diagonal 645, 08028 Barcelona, Spain.

[B]Centre National de la Recherche Scientifique, UPR 2357, Institut de Biologie Moléculaire des Plantes, 28 rue Goethe, 67083 Strasbourg Cedex, France.

[C]Present address: Universidad Autónoma de Chile-Sede Talca, Escuela de Ciencias de la Salud, 5 Poniente Número 1670, Talca, Chile.

[D]Present address: Centre de Recerca en Agrigenòmica (CRAG-CSIC), Jordi Girona 18-26, 08034 Barcelona, Spain.

[E]Corresponding author. Email: aboronat@ub.edu

Abstract. Thiolases are ubiquitous enzymes involved in many essential biochemical processes. Biosynthetic thiolases, also known as acetoacetyl-CoA thiolases (AACT), catalyse a reversible Claisen-type condensation of two acetyl-CoA molecules to form acetoacetyl-CoA. Here, we report the characterisation of two genes from *Arabidopsis thaliana* L., *ACT1* and *ACT2,* which encode two closely related AACT isoforms (AACT1 and AACT2, respectively). Transient expression of constructs encoding AACT1 and AACT2 fused to GFP revealed that the two proteins show a different subcellular localisation. While AACT1 is found in peroxisomes, AACT2 localises in the cytosol and the nucleus. The peroxisomal localisation of AACT1 depends on the presence of a C-terminal peroxisomal targeting sequence (PTS1) motif (Ser-Ala-Leu) not previously found in other organisms. *ACT1* and *ACT2* genes are also differentially expressed. Whereas *ACT2* is expressed at relatively high level in all plant tissues, the expression of *ACT1* is restricted to roots and inflorescences and its transcript is present at very low levels. The obtained results are in agreement with the involvement of AACT2 in catalysing the first step of the mevalonate pathway. The metabolic function of AACT1 is not clear at present, although its particular peroxisomal localisation might exclude a role in isoprenoid biosynthesis.

Additional keywords: acetyl-CoA, isoprenoid biosynthesis, mevalonate pathway, peroxisome.

Introduction

Thiolases include a family of ubiquitous enzymes involved in many vital biochemical pathways. According to their enzymatic activities, thiolases have been divided into two groups: biosynthetic thiolases and degradative thiolases (Igual *et al.* 1992; Peretó *et al.* 2005). Although this division is based on the original description of their biological functions, the main biochemical feature differentiating the enzymes included in each group is the substrate specificity. Biosynthetic thiolases, also known as acetoacetyl-CoA thiolases (AACT) (EC 2.3.1.9), catalyse a Claisen-type condensation of two acetyl-CoA molecules to form acetoacetyl-CoA. Degradative thiolases, also known as 3-oxoacyl-CoA thiolases (OACT) (EC 2.3.1.16), have a broad substrate specificity and catalyse the thiolytic cleavage of 3-oxoacyl-CoAs of different lengths to yield acetyl-CoA and shortened acyl-CoA species. Despite biosynthetic and degradative thiolases only showing a sequence identity of ~38%, crystallographic data have revealed that all of them have the same folding and that the differences in substrate specificity mainly reflect the size of the substrate binding pocket in the active site (Mathieu *et al.* 1997; Modis and Wierenga 2000). In the degradative thiolases, the active site pocket is large enough to accommodate long chain fatty acids, while in biosynthetic thiolases, the binding pocket is much smaller and only accommodates smaller substrates. Kinetic analyses have shown that the reaction catalysed by thiolases is reversible, although the equilibrium of the reaction is in favour of the cleavage direction (Gilbert *et al.* 1981). Thus, the metabolic role of a particular thiolase will largely depend on the substrate(s) available in a particular cell type or subcellular compartment.

OACT is known to play a key role in the β-oxidation cycle linked to the catabolism of fatty acids (Kunau *et al.* 1995). In agreement with this, eukaryotic OACTs are localised in peroxisomes and mitochondria. In plants, OACTs have been extensively characterised because of their essential role in the mobilisation of storage lipids during seed germination (Graham and Eastmond 2002). Peroxisomal (and glyoxysomal) OACTs have been cloned from *Arabidopsis thaliana* L., *Brassica*

napus L., *Cucumis sativus* L., *Helianthus annuus* L., *Mangifera indica* L. and *Cucurbita* sp. (Bojorquez and Gómez-Lim 1995; Kato *et al.* 1996; Olesen *et al.* 1997; Hayashi *et al.* 1998; Schiedel *et al.* 2004). All plant OACTs characterised so far contain an N-terminal transit peptide for targeting into peroxisomes (PTS2) (Schiedel *et al.* 2004).

In animal cells, biosynthetic AACT activity can be found in the cytosol and the mitochondria. Cytosolic AACT provides acetoacetyl-CoA for the synthesis of sterols and other isoprenoids (via the mevalonate pathway), whereas mitochondrial AACT produces the acetoacetyl-CoA used for the synthesis of ketone bodies. Recently, a peroxisomal AACT, presumably involved in cholesterol biosynthesis, has also been described in mammalian cells (Olivier and Krisans 2000). In prokaryotic organisms AACT is known to participate in the synthesis of polyhydroxyalkanoates (Madison and Huisman 1999). The reverse (degradative) reaction of AACT has been described in the β-oxidation of fatty acids (Kunau *et al.* 1995; Kanayama *et al.* 1998) and in the metabolism of leucine and ketone bodies (Antonenkov *et al.* 2000).

In spite of the well established role of AACT in the synthesis of isoprenoids in different organisms, relatively little is known about this enzyme in plants (Vollack and Bach 1996; Bach *et al.* 1999). Isoprenoids, also known as terpenoids, are ubiquitous compounds found in all living organisms. In plants, isoprenoids have essential roles in membrane architecture (sterols), photosynthesis (carotenoids and chlorophylls), electron transport (plastoquinone, ubiquinone), glycosylation (dolichol) and growth regulation (gibberellins, abscisic acid, brassinosteroids and cytokinins). Although the role of other plant isoprenoids is less evident, like that of the vast array of secondary metabolites, some are known to play key roles in the adaptive responses to different environmental challenges (Chappell 1995; Croteau *et al.* 2000; Bouvier *et al.* 2005).

Five genes encoding thiolases have been annotated in the *Arabidopsis* genome: *At2g33150*, *At1g04710*, *At5g48880*, *At5g48230* and *At5g47720* (http://www.tigr.org, accessed 8 January 2008). *At2g33150*, *At1g04710*, *At5g48880* correspond to the previously characterised *PED1*/*KAT2*, *KAT1* and *KAT5*/*PKT1–2* genes, respectively, encoding peroxisomal OACTs (Hayashi *et al.* 1998; Germain *et al.* 2001; Graham and Eastmond 2002; He *et al.* 2002; Castillo *et al.* 2004). *At5g47720* and *At5g48230* encode putative AACTs. The subcellular localisation of different isoforms predicted to be encoded by *At5g47720* and *At5g48230* has recently been reported (Carrie *et al.* 2007). However, the biochemical function and metabolic role of the *At5g47720* and *At5g48230* gene products have not yet been described. This report shows that the *At5g47720* and the *At5g48230* genes (designated as *ACT1* and *ACT2*, respectively) are differentially expressed and encode functional AACT isoforms (designated as AACT1 and AACT2) showing differential subcellular localisation. The proposed metabolic role of AACT1 and AACT2 is discussed.

Materials and methods

Plant material and treatments

All biological materials used in this work were derived from *Arabidopsis thaliana* L. plants of the ecotype Columbia. Plants were grown under 16 h light/8 h dark illumination regime as previously described (Cunillera *et al.* 1996). Roots were obtained from three-week-old plants grown on filter papers layered onto Murashige and Skoog (MS) medium supplemented with 1% (w/v) sucrose and 2% (w/v) agar.

Isolation of cDNA clones

Clones were isolated from a cDNA library prepared from tissue-cultured roots, etiolated seedlings and rosette leaves from *Arabidopsis*. The library was screened according to standard protocols using the entire radish AACT cDNA sequence (Vollack and Bach 1996) as a probe. Hybridisation of the replica filters (nitrocellulose; Millipore, Bedford, MA, USA) was performed at 65°C for 18 h in 6 × SSC, 2 × Denhardt's and 100 μg mL^{-1} of denatured salmon sperm DNA. The filters were washed twice at 65°C in 6 × SSC for 15 min, twice at 45°C in 2 × SSC, 0.1% SDS for 20 min, and twice at 45°C in 0.2 × SSC, 0.1% SDS for 20 min. The insert of the positive clones was subcloned into plasmid pBluescript and sequenced.

Rapid amplification of cDNA ends (RACE)

The 5′ and 3′ ends of the mRNAs encoding AACT1 and AACT2 were amplified with the 5′-RACE and 3′-RACE systems from Life Technologies/GibcoBRL (Gaithersburg, MD, USA), following the recommendations of the supplier. One microgram of total RNA from 12-day-old *Arabidopsis* seedlings was used as a template in both cases. For the *ACT1* transcripts, oligonucleotides ACT1R5′ and ACT1R3′ (Table 1) were used as primers for 5′-RACE and 3′-RACE experiments, respectively. For the *ACT2* mRNA, oligonucleotides ACT2R5′-1 and ACT2R5′-2 were the specific antisense primers in the 5′-RACE (Table 1). Primer ACT2R5′-1 was used in the starting reverse transcription reaction. Oligonucleotide ACT2R5′-2 was used in the final PCR reaction. Oligonucleotide ACT2R3′-1 was used as the specific sense primer in the PCR reaction of the 3′-RACE.

Heterologous expression of AACT1 and AACT2 in Escherichia coli and enzyme assays

The coding regions of *AACT1* and *AACT2* cDNAs were amplified by PCR (*Pfu* DNA polymerase) using the sets of primers AACT1(NdeI)/AACT1(*Bam*HI) and AACT2(NdeI)/AACT2(*Bam*HI) (Table 1) and cloned into the *Sma*I site of plasmid pBluescript to generate plasmids pBS-AACT1 and pBS-AACT2, respectively. After digestion of plasmids pBS-AACT1 and pBS-AACT2 with NdeI and *Bam*HI, the excised inserts were purified by agarose gel electrophoresis and cloned into the corresponding restriction sites of the expression plasmid pET23b(+) to generate plasmids pET23-AACT1 and pET23-AACT2, respectively The resulting constructs encode the corresponding AACT proteins containing a short C-terminal extension with a His × 6 tag. Plasmids pET23-AACT1 and pET23-AACT2 were checked by DNA sequencing. A derivative of plasmid pET23-AACT1 encoding an inactive version of AACT1 containing a mutation in the Cys residue at position 99 was used as a negative control.

Table 1. Oligonucleotides used in this study

Name	Sequence
AACT1(*Bam*HI)	5′-TATTAGGATCCGAGTGCCGAATATCCGATTG-3′
AACT1(NdeI)	5′-TGACTCATATGGCTCCGCCTGTCTCTG-3′
AACT1f	5′-CATAATTTCTTCGGTGACTTCC-3′
AACT1r	5′-CACACATGAACCATATACATAAG-3′
AACT2(*Bam*HI)	5′-CATAATGGATCCAAGGAGCTCAAGAACTAGAGCAG-3′
AACT2(NdeI)	5′-AGATTACATATGGCCCATACATCAGAATCTG-3′
ACT1R3′	5′-CAACAGTATCATGACCTAATCG-3′
ACT1R5′	5′-ATGTCGGAGAAGACAATCGGA-3′
ACT2R3′-1	5′-TGCAACGGAGGAGGAGGTGCT-3′
ACT2R5′-1	5′-CAGATAACAGAGTTAGGGATTCCT-3′
ACT2R5′-2	5′-CCAAGCTTTGTGGCAGGTAA-3′
CATf	5′-CGCATCACGCATGAGCTCCGCAGTATCTGG-3′
CATr	5′-GGCCAATCTAGAATTCTTTCACTCGTT-3′
NLS-1	5′-CTTGGGATACTAAACAACAGCAACGGAAAGTACGG-3′
NLS-2	5′-CCGTACTTTCCGTTGCTGTTGTTTAGTATCCCAAG-3′
p121	5′-GGGTTGGATACAGTAATTTAA-3′
p355	5′-CGACCCACCCACCATATATT-3′
p906	5′-GAGACCAGTCAAAGAACCACTT-3′
pCS15	5′-GGATTCACGGATCCTGATGT-3′
SALf	5′-CTTCATGTCGGAGAAGACAATCGGATATTCGGCA-3′
SALr	5′-CTAGTCAGAGTGCCGAATATCCGATTGTCTTCTCCGACATGAAGAGCT-3
SALmutf	5′-CTTCATGTCGGAGAAGACAATCGGATATGGAGATGGTTGA-3′
SALmutr	5′-CTAGTTCAACCATCTCCATATCCGATTGTCTTCTCCGACATGAAAGAGCT-3′
T2	5′-GGGCGAGCCACTAGGCATGCTCCAGGTGACTG-3′
T20	5′-GGCTGTAGGGAATCAGAGACACCCGGGGCCATGGAAGTCACCG-3′

Overnight cultures of Rosetta-gami *Escherichia coli* cells (Novagen, Madison, WI, USA) harbouring the corresponding expression plasmids were diluted 100-fold in LB medium containing 100 $\mu g\,mL^{-1}$ ampicillin and incubated at 22°C. When the OD_{600} reached 0.5, protein expression was induced by adding isopropyl-β-D-thiogalactoside (final concentration 0.5 mM) and incubation for 16 h. Cells were collected by centrifugation, broken in liquid nitrogen using a mortar and homogenised in 100 mM TRIS-HCl pH 8.0 containing 5 mM β-mercaptoethanol. The supernatant following centrifugation at 10 000*g* (20 min at 4°C) was used as source of the enzyme. Based on the technique described by Clinkenbeard *et al*. (1973), thiolase activity was assayed in 1 mL (total volume) of 100 mM TRIS-HCl, pH 8.0, 0.1 mM EDTA, 50 mM $MgCl_2$, 120 μM acetoacetyl-CoA and 90 μM CoA. Product formation was followed by quantifying the decrease of the absorbance at 302 nm (A_{302}, ε = 16 100) corresponding to the loss of the enol absorption band of Mg-acetoacetyl-CoA. The mixture was stabilised at 23°C and an appropriate amount of total protein extract was used to start the enzyme-catalysed reaction.

The expressed AACT proteins were identified by western-blotting using an anti-His_6 antibody (Roche Diagnostics, Mannheim, Germany) following the manufacturer's instructions. Because His-tagged AACTs were not retained at significant level by the Ni^{+2} matrix, the protein concentration corresponding to each enzyme was quantified after SDS–PAGE and Coomassie blue staining of total soluble proteins using pixel quantification with Image J software (http://rsb.info.nih.gov/ij/, accessed 23 September 2004). Different amounts of BSA migrating in parallel were used as standards.

RNA isolation and northern blot analysis

Total RNA from seedlings or different organs from *Arabidopsis* was isolated as described (Dean *et al.* 1985). Twenty micrograms of RNA per sample were fractionated in a 1% (w/v) agarose gel containing 2.2 M formaldehyde and transferred onto a nylon Hybond-N^+ membrane (Amersham, Uppsala, Sweden). Ethidium bromide staining of the gel before transfer showed that equivalent amounts of RNA were present in each lane. Hybridisation was performed using a 260 bp PCR fragment corresponding to the 3′-untranslated region (UTR) of the *ACT1* mRNA and a 120 bp *Eco*RI cDNA fragment corresponding to the 5′-UTR of the *ACT2* mRNA as probes. Previous experiments of Southern blot showed that these probes were gene-specific. Filters were hybridised for 2 h at 65°C in ExpressHyb hybridisation solution (Clontech, Heidelberg, Germany) and washed twice at room temperature in 2 × SSC for 15 min, 0.5% SDS, twice at 65°C in 2 × SSC, 0.5% SDS for 20 min and twice at 65°C in 0.1 × SSC for 20 min.

Constructs for plant transformation

A 3.8 kbp *Eco*RI fragment corresponding to the 5′-region of the *ACT1* gene was cloned in the pBluescript plasmid. A PCR reaction using primers T20 (antisense) and T2 (sense) (Table 1) allowed the amplification of a fragment from the 3.8 kbp insert that contained 1097 bp of the 5′-flanking region, the whole 5′-UTR, and 9 bp of the coding sequence. The PCR fragment was cloned into plasmid pGEM-T (Promega, Madison, WI, USA) in the appropriate orientation to recover the insert by digestion with the appropriate restriction enzymes The inserts

were cloned into plasmid pBI121 (Jefferson 1987) previously digested with the same restriction enzymes to remove the CaMV35S promoter. The obtained constructs were analysed by DNA sequencing.

A 3.6 kbp *Hind*III fragment of the *ACT2* gene was cloned in the pBluescript plasmid. This fragment contains 3.3 kbp of the 5′-flanking region and the first two exons of the gene. A series of PCR reactions allowed the amplification of fragments that contained various extensions of the 5′-flanking region, the whole 5′-UTR and 15 bp of the coding sequence. The antisense primer pCS15 (Table 1), which determined the downstream limit of the constructs, was common to all PCR reactions. This oligonucleotide introduced a *Bam*HI restriction site in the sequence. The sense primers p906, p355 and p121 (Table 1), which determined the upstream limit of the constructs, were specific for each reaction. The PCR fragments were cloned into plasmid pGEM-T (Promega), in the appropriate orientation to recover the insert by digestion with *Bam*HI and *Pst*I. The inserts were cloned into plasmid pBI221 (Jefferson 1987) previously digested with the same restriction enzymes to remove the CaMV35S promoter. The CaMV35S-*GUS* expression unit of plasmid pBI121 was replaced by the *ACT2*:*GUS* fusions of the pBI221 derivatives, for the generation of transgenic plants. The obtained constructs were analysed by DNA sequencing.

Plant transformation and histochemical analysis of transgenic plants

Transgenic *Arabidopsis* plants were obtained with the *in planta* transformation method described by Bechtold *et al*. (1993). Previously, constructs were introduced into *Agrobacterium tumefaciens* strain C58C1 (pGV2260) as reported (An 1986). Inflorescences of *Arabidopsis* plants (generation T_0) were vacuum infiltrated with the transformed *A. tumefaciens* strains. Seeds of these plants were harvested, surface sterilised and sown in Petri dishes containing MS solid medium supplemented with 0.5 mg mL^{-1} MES pH 5.7, 10 mg mL^{-1} sucrose and 50 μg mL^{-1} kanamycin. Seedlings resistant to kanamycin (generation T_1) were transferred to soil and grown to maturity. Histochemical analysis of GUS activity was performed in transgenic plants (T_2) of ~10 independent lines for each construct. GUS staining was performed by immersing the plant material in 50 mM sodium phosphate pH 7.0, containing 1 mg mL^{-1} 5-bromo-4-chloro-3-indolyl β-D-glucuronide (X-gluc). Samples were subjected to vacuum for 5 min and incubated at 37°C for 2 to 16 h. To improve the contrast of staining, chlorophyll was removed by extensive washing with 70% (v/v) ethanol.

Micro-bombardment assays and analysis of the subcellular localisation of AACT1 and AACT2

The region encoding AACT1 was amplified by PCR using primers AACT1f and AACT1r (Table 1). The PCR product was digested with *Sac*I and *Xba*I and cloned into plasmid pGFP-MRC (Rodríguez-Concepción *et al.* 1999) previously digested with the same restriction enzymes. The resulting construct encodes the entire AACT1 protein fused to the C-terminus of GFP (GFP-AACT1). A construct encoding the last 12 amino acid residues of AACT1 fused to the C-terminus of GFP (GFP-SAL) was generated in the same way but using primers SALf and SALr (Table 1). A construct encoding a mutated version of GFP-SAL in which the C-terminal SerAlaLeu motif was replaced by GlyAspGly (GFP-SALmut) was generated in the same way than pGFP-SAL but using primers SALmutf and SALmutr (Table 1). A construct encoding the last 49 amino acid residues of catalase 2 from *Arabidopsis* fused to the C-terminus of GFP was generated in the same way using primers CATf and CATr (Table 1).

A 1.3 kbp *Bam*HI-*Bgl*II fragment containing the entire coding sequence of the cDNA encoding AACT2 was ligated to the same sites of plasmid pGFP-MRC. The resulting construct encodes the AACT2 protein fused to the C-terminus of GFP. The nuclear localisation sequence (NLS) of GFP-AACT2 was removed with the Site-Directed Mutagenesis Kit from Stratagene (Heidelberg, Germany), using oligonucleotides NLS-1 and NLS-2 as mutagenic primers. The resulting chimeric protein was named GFP-AACT2-NLSmut.

Leaves from 15-day-old *Arabidopsis* seedlings and onion (*Allum cepa* L.) epidermal cells were micro-bombarded with tungsten particles (1.0 μm) coated with plasmid DNA, using the Biolistic PDS-1000/He system (Bio-Rad, Irving, CA, USA) at a pressure of 1100 psi. Samples were incubated at 22°C for 24 h with continuous light and examined with a Leica TCS 4D or SP2 Confocal Laser Scanning Microscopes. The green and red fluorescence corresponding to GFP and RFP was detected by excitation at 488 and 543 nm, respectively.

Results

Identification and characterisation of cDNA clones encoding AACT1 and AACT2 in Arabidopsis

A radish cDNA sequence encoding cytosolic AACT (Vollack and Bach 1996) was used as a probe to identify homologous sequences from an *Arabidopsis* cDNA library (for details, see Materials and methods). Three positive clones were isolated and sequenced. The cDNAs, which only differed in the length of the 5′- and 3′-UTR contained an open reading frame of 1209 nucleotides encoding a protein of 403 amino acid residues with a deduced molecular mass of 41.4 kDa. This protein shows 92% identity (94% similarity) with the cytosolic AACT from radish reported by Vollack and Bach (1996). The cloned cDNA corresponds to a transcript encoded by the *At5g48230* locus. Since *Arabidopsis* contains a second annotated locus encoding a putative AACT (*At5g47720*), the corresponding cDNA was cloned by reverse transcription (RT)–PCR using primers designed from the genomic sequence. The isolated cDNA has an open reading frame of 1245 nucleotides which encodes a protein of 415 amino acid residues with a deduced molecular mass of 43.2 kDa. The proteins encoded by *At5g47720* and *At5g48230* show 78% identity and 90% similarity (Fig. 1). In agreement with previous reports (Lange and Ghassemian 2003; Wille *et al.* 2004; Jin and Nikolau 2007) the proteins encoded by *At5g47720* and *At5g48230* were designated as AACT1 and AACT2, respectively.

The 5′-end of the mRNAs encoding AACT1 and AACT2 was identified by 5′-RACE. The 5′-end of the transcript encoding AACT2 was mapped 184 nucleotides upstream of the translation start site. In the case of AACT1, two populations of transcripts having the same 5′-end but differing by the presence or absence of an exon of sequence 83 nucleotides in the 5′-UTR (at position

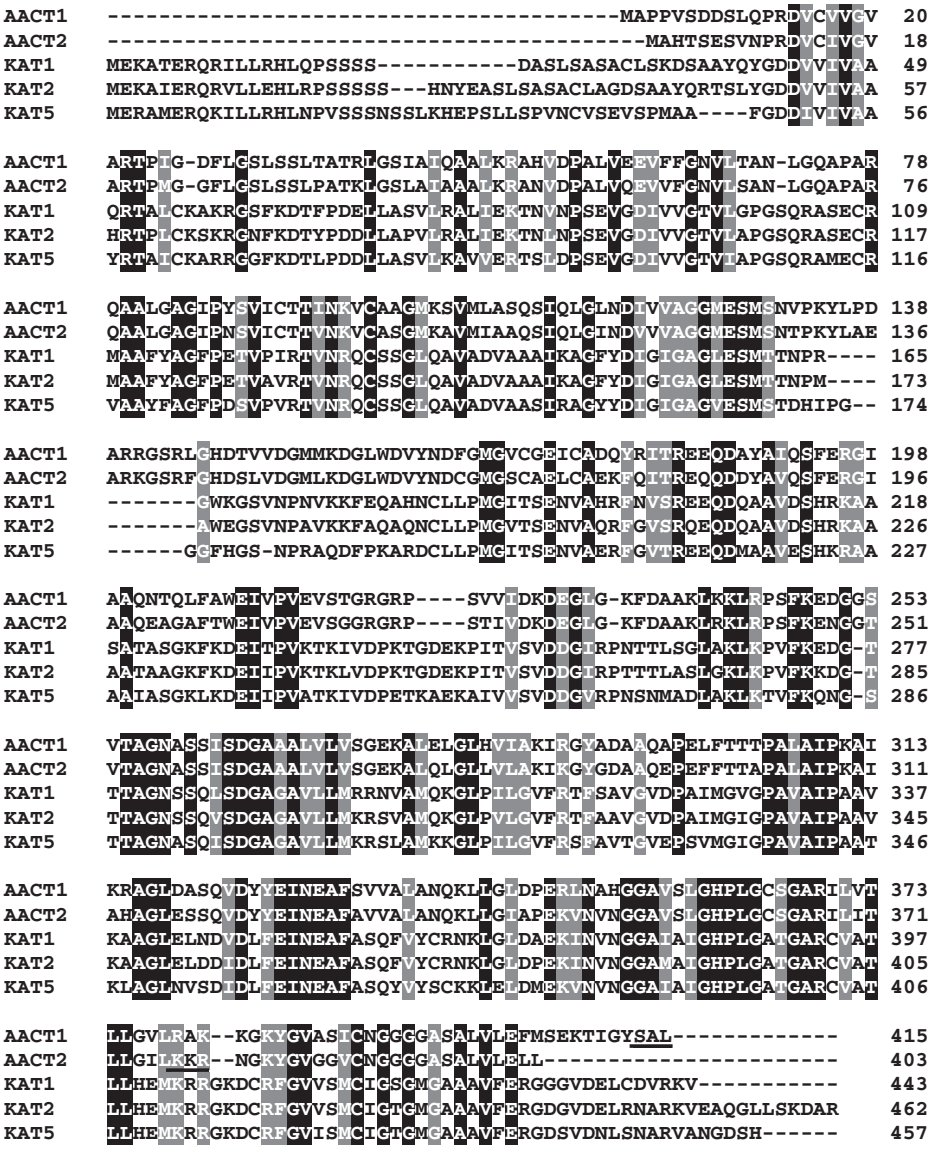

Fig. 1. Alignment of AACT1 and AACT2 with peroxisomal 3-oxoacyl-CoA thiolases (OACTs) from *Arabidopsis thaliana* L. ecotype Columbia-3. AACT1 and AACT2 correspond to the annotated *At5g47720* and *At5g48230* gene products, respectively. KAT1, KAT2 and KAT5 correspond to peroxisomal OACTs previously characterised in *Arabidopsis* (*At1g04710*, *At2g33150* and *At5g48880,* respectively). The amino acid sequences are numbered on the right. White letters on black background indicate residues identical in all five proteins. White letters on grey background indicate conserved residues. The peroxisomal targeting sequence (SAL) present at the C-terminal end of AACT1 and the nuclear localisation signal identified in AACT2 (residues 377–379) are underlined.

+71) were detected. The length of the 5′-UTRs was 176 and 93 nucleotides, respectively. Both transcripts, however, contain the same open reading frame. 3′-RACE experiments showed heterogeneity in the position of the polyadenylation tail of the mRNAs encoding AACT1 and AACT2.

Arabidopsis *AACT1 and AACT2 cluster with biosynthetic thiolases in phylogenetic analysis*

To better represent the relationship of AACT1 and AACT2 with previously identified thiolases, a phylogenetic tree was constructed (Fig. 2). Four main groups can be distinguished. Group I includes fungal cytosolic thiolases that catalyse the first step of the mevalonate (MVA) pathway, mammalian mitochondrial thiolases involved in ketone body metabolism, the radish cytosolic AACT, and the cloned *Arabidopsis* AACT1 and AACT2 proteins. Group II includes prokaryotic thiolases that catalyse the first step of the polyhydroxyalkanoate biosynthetic pathway and eukaryotic cytosolic thiolases involved in the MVA pathway. Group III is formed by degradative thiolases of eukaryotic and prokaryotic origin catalysing sequential steps of the fatty acid β-oxidation cycle. This is the most

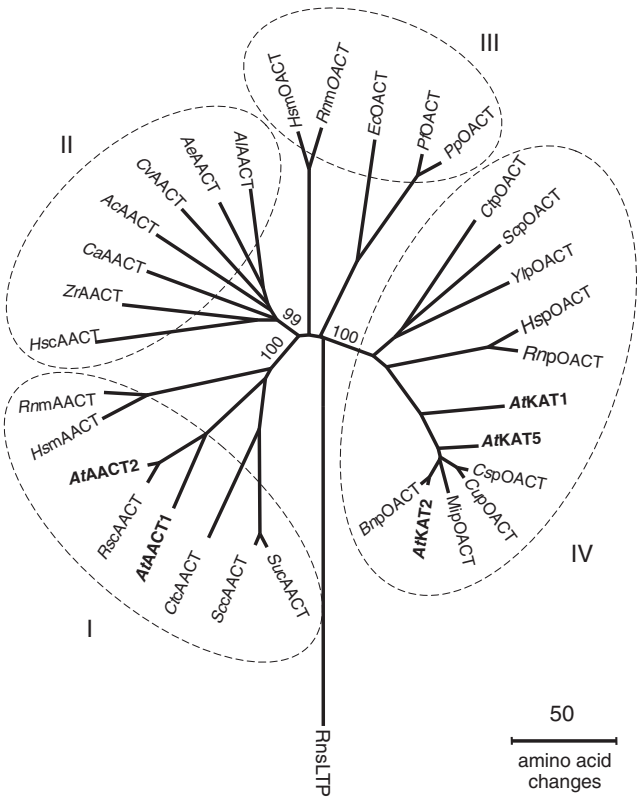

Fig. 2. Phylogenetic analysis of thiolases. The evolutionary tree was constructed with the neighbour-joining method of the program MEGA 2.0 (http://www.megasoftware.net), using the number of amino acid differences as a distance. The N-terminal region (400 residues) of the rat liver non-specific lipid-transfer protein (RnsLTP) was used as outgroup, as in a previous work (Igual *et al.* 1992). Those sites in which a least one of the sequences displayed a deletion were removed. The bootstrap procedure (Felsenstein 1985) was applied to determine the consistency of the analysis. The branching points leading to groups I, II and IV were found highly significant. They occurred in 99 or 100% of 1000 bootstrap replicates, as indicated. In all cases, the first two letters correspond to the organism from which the sequence is derived: *Ac*, *Acinobacter* sp.; *Ae*, *Alcaligenes eutrophus*; *Al*, *Alcaligenes latus*; *At*, *Arabidopsis thaliana* L.; *Bn*, *Brassica napus* L.; *Ca*, *Clostridium acetobutylicum*; *Cv*, *Chromatium vinosum*; *Cs*, *Cucumis sativus* L.; *Ct*, *Candida tropicalis*; *Cu*, *Cucurbita* sp.; *Ec*, *Escherichia coli*; *Hs*, *Homo sapiens*; *Mi*, *Mangifera indica* L.; *Pf*, *Pseudomonas fragi*; *Pp*, *Pseudomonas putida*; *Rn*, *Rattus norvegicus* L.; *Rs*, *Raphanus sativus* L.; *Sc*, *Saccharomyces cerevisae*; *Su*, *Saccharomyces uvarum*; *Yl*, *Yarrowia lipolytica*; *Zr*, *Zooglea ramigera*. The last four letters indicate the enzymatic activity: AACT, acetoacetyl-CoA thiolase; OACT, 3-oxoacyl-CoA thiolase. In the name of eukaryotic sequences, the third letter indicates the subcellular location: c, cytosolic; m, mitochondrial; p, peroxisomal. The *Arabidopsis* proteins AACT1, AACT2, KAT1, KAT2 and KAT5 are indicated in bold.

heterogeneous group in the evolutionary tree. Thiolases of group IV also catalyse steps within the β-oxidation cycle, but all of them stem from eukaryotic organisms (including plants) and are found in peroxisomes. The phylogenetic tree reflects an overall separation between the putative biosynthetic thiolases of groups I and II and the degradative thiolases of groups III and IV. It is worth noting that the branching points leading to the sequences of groups I, II and IV are highly significant according to the bootstrap test (Fig. 2). In particular, there is a very significant phylogenetic distance between the plant thiolases of group I and those of group IV. At first view, the clustering of *Arabidopsis* AACT1 and AACT2 with the biosynthetic thiolases of group I suggests that these enzymes could be involved in isoprenoid biosynthesis.

Arabidopsis *AACT1 and AACT2 show AACT activity*

The functional characterisation of AACT1 and AACT2 was accomplished by expression in *E. coli* and measuring AACT activity in the cell extracts (for details, see Materials and methods). An inactive version of AACT1, carrying a mutation in the essential Cys residue located at position 99, corresponding to Cys89 in AACT from *Zoogloea ramigera* (Modis and Wierenga 2000), was used as a negative control. The results shown in Fig. 3 indicate that *Arabidopsis* AACT1 and AACT2 are expressed as soluble active enzymes and that the estimated specific activity is similar for the two isozymes.

Arabidopsis *AACT1 and AACT2 show a different subcellular localisation*

To study the subcellular localisation of AACT1 and AACT2 their coding sequences were fused in frame with the sequence encoding an improved version of the Green Fluorescent Protein (GFP) (Rodríguez-Concepción *et al.* 1999). The constructs were introduced into epidermal cells of 15-day-old *Arabidopsis* seedlings or onion epidermal cells through particle bombardment and fluorescence analysed by confocal laser scanning microscopy.

In the case of GFP-AACT1, fluorescence was observed as a punctate pattern (Fig. 4*A*) equivalent to that of GFP fused to the 49 C-terminal amino acid sequence of catalase-2 (data not shown), a known marker for plant peroxisomes (Zhong *et al.* 1994; Frugoli *et al.* 1996). To confirm that GFP-AACT1 was actually targeted to peroxisomes, co-localisation studies using a monomeric Red Fluorescent Protein (RFP) derivative harbouring a peroxisomal targeting sequence (Hemmerlin *et al.* 2006) were performed. The results shown in Figs 4*D–F* clearly show that GFP-AACT1 co-localises with the peroxisomal targeted RFP protein.

The peroxisomal location of AACT1 was not surprising since the protein has a C-terminal extension with respect to AACT2 and cytosolic radish AACT showing features of a C-terminal peroxisomal targeting sequence (PTS1, see Fig. 1) (Hayashi *et al.* 1997). To confirm the involvement of this sequence in the subcellular localisation of AACT1, the last 12 C-terminal amino acid residues of the protein were fused to GFP to generate construct GFP-SAL. As shown in Fig. 4*B*, fluorescence also displayed the punctate pattern previously observed for GFP-AACT1. A derivative construct in which the Ser-Ala-Leu sequence was changed to Gly-Asp-Gly (construct GFP-SALmut) showed a cytosolic distribution (Fig. 4*C*). Together, these results demonstrate that AACT1 carries a functional PTS1 for peroxisomal localisation. The nuclear localisation of GFP-SAL and GFP-SALmut (Figs 4*B*, *C*) was the result of the diffusion of these proteins through the nuclear pore complex, which has a size exclusion limit of ~40–60 kDa (Köhler 1998). In agreement

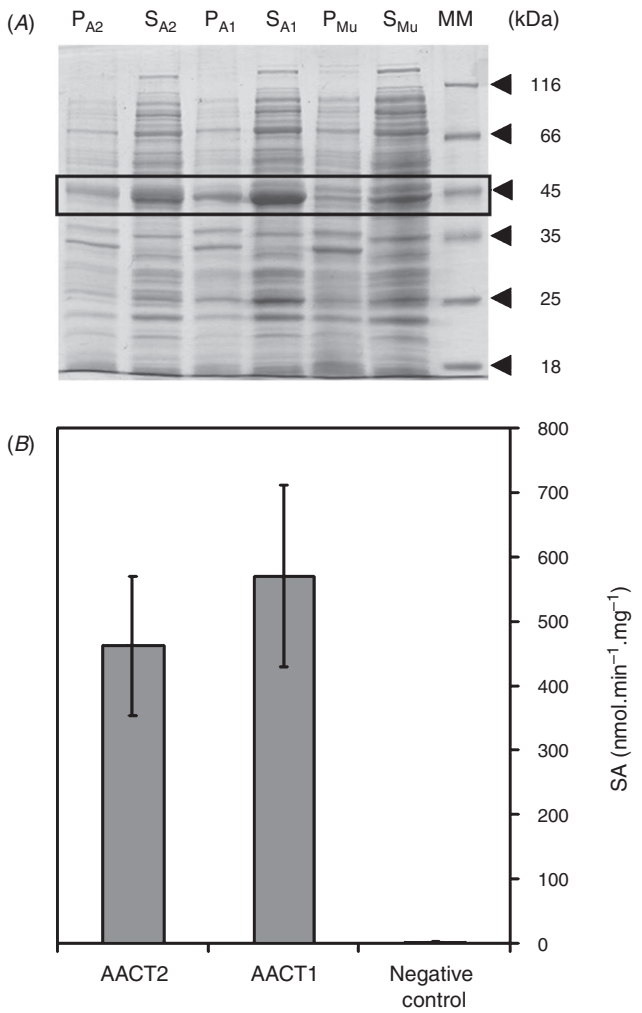

Fig. 3. Functional analysis of *Arabidopsis thaliana* L. ecotype Columbia-3 AACT1 and AACT2. *Escherichia coli* cell-free extracts and AACT assays were performed as described under Materials and methods. (*A*) Pattern of bands obtained after SDS–PAGE and Coomassie-blue staining of the pellet (P) and supernatant (S) fractions of *E. coli* extracts corresponding to the expression of AACT1 (A1), AACT2 (A2), and the mutant (inactive) form of AACT1 (Mu), used as a negative control. The region of the gel containing the expressed AACT proteins is indicated. The position and the molecular weight of the protein markers (MM) used are shown on the right side. (*B*) Specific activities (SA) of AACT1, AACT2 and AACT1 (Mu) (negative control) expressed in nmol $min^{-1}.mg^{-1}$ of AACT protein contained in the crude extract. Standard deviations are indicated in the diagram. The whole procedure (*E. coli* transformation, enzyme production, protein extraction and enzyme assays) was performed three times.

with this, control non-fused GFP was also detected in the cytosol and the nucleus (Fig. 4*G*).

GFP-AACT2 protein accumulated in the cytosol and nucleus (Fig. 4*H*). Although the presence of GFP-AACT2 in the cytosol is consistent with the role of AACT2 in the MVA pathway, the accumulation of GFP-AACT2 in the nucleus was unexpected considering the large size of the chimeric protein (Köhler 1998). Inspection of the AACT2 amino acid sequence for the presence of nuclear localisation signals (NLS), which typically consist in short polypeptide regions rich in basic residues (Raikhel 1992), revealed a stretch of basic amino acids (Lys-Lys-Arg) at positions 377 to 379 of the protein (Fig. 1). To determine whether this putative NLS was indeed responsible for the nuclear targeting of AACT2, a construct encoding a derivative of GFP-AACT2 in which the Lys-Lys-Arg sequence was changed to Asn-Asn-Ser was generated. The new fusion protein, named GFP-AACT2-NLSmut, was exclusively found in the cytosol (Fig. 4*I*), indicating that the Lys-Lys-Arg sequence is required for the observed targeting of GFP-AACT2 to the nucleus.

At5g48230 *and* At5g47720 *are differentially expressed*

The expression pattern of *At5g47720* and *At5g48230*, hereafter referred to as *ACT1* and *ACT2* respectively, was first studied by northern blot analysis using total RNA isolated from seedlings, stems, rosette leaves, inflorescences and roots. Gene-specific probes corresponding to the 3′-UTR of the *ACT1* mRNA and to the 5′-UTR of the *ACT2* mRNA were used for hybridisation (for details, see Materials and methods). A transcript of ~1.6 kb corresponding to the *ACT2* gene was detected at similar levels in all RNA samples indicating that the gene is constitutively expressed (data not shown). In contrast, the *ACT1* transcript was hardy detected by RNA gel blot analysis. Only after long exposures a transcript of ~1.6 kb could be observed in the RNA samples corresponding to roots and inflorescences (data not shown).

To further characterise the *ACT1* and *ACT2* gene expression pattern, *Arabidopsis* transgenic plants carrying a translational fusion between the 5′-flanking region of the *ACT1* or the *ACT2* genes and the entire coding sequence of the *GUS* reporter gene were generated.

For the *ACT1* gene, transgenic plants harbouring a construct containing the region extending from nucleotide −1097 to +184 fused to the GUS reporter gene (construct [−1097/+184]*ACT1*::*GUS*) were generated (coordinate +1 corresponds to the transcription start site of the longest *ACT1* transcript determined by 5′-RACE). Histochemical analysis of the transgenic plants revealed an almost undetectable GUS staining during vegetative and reproductive growth. Only after long incubations periods (more than 40 h) a faint and diffuse staining was observed in roots and inflorescences (data not shown), in agreement with the results obtained by northern blot.

To study the expression of the *ACT2* gene, a construct containing 1197 bp extending from nucleotides −906 to +291 (coordinate +1 corresponds to the transcription start site determined by 5′-RACE) was first used (construct [−906/+291]*ACT2*::*GUS*). Although some variation in the intensity of GUS staining was observed among the different transgenic lines, all of them showed the same expression pattern. GUS staining was detected in the germinating seedlings as soon as they emerged from the seed (Fig. 5*A*). In the first stages of development, GUS activity was high in the cotyledons, particularly in the vascular tissue, the hypocotyl and the root (Fig. 5*A*). After the first true leaves appeared, GUS levels declined in the stem and leaves (Fig. 5*B*). The staining was progressively restricted to the vascular tissue of basal and cauline leaves (Fig. 5*B*, *C*). In contrast, high GUS activity was maintained in roots (Fig. 5*B*). In stems, GUS activity was mainly restricted to the

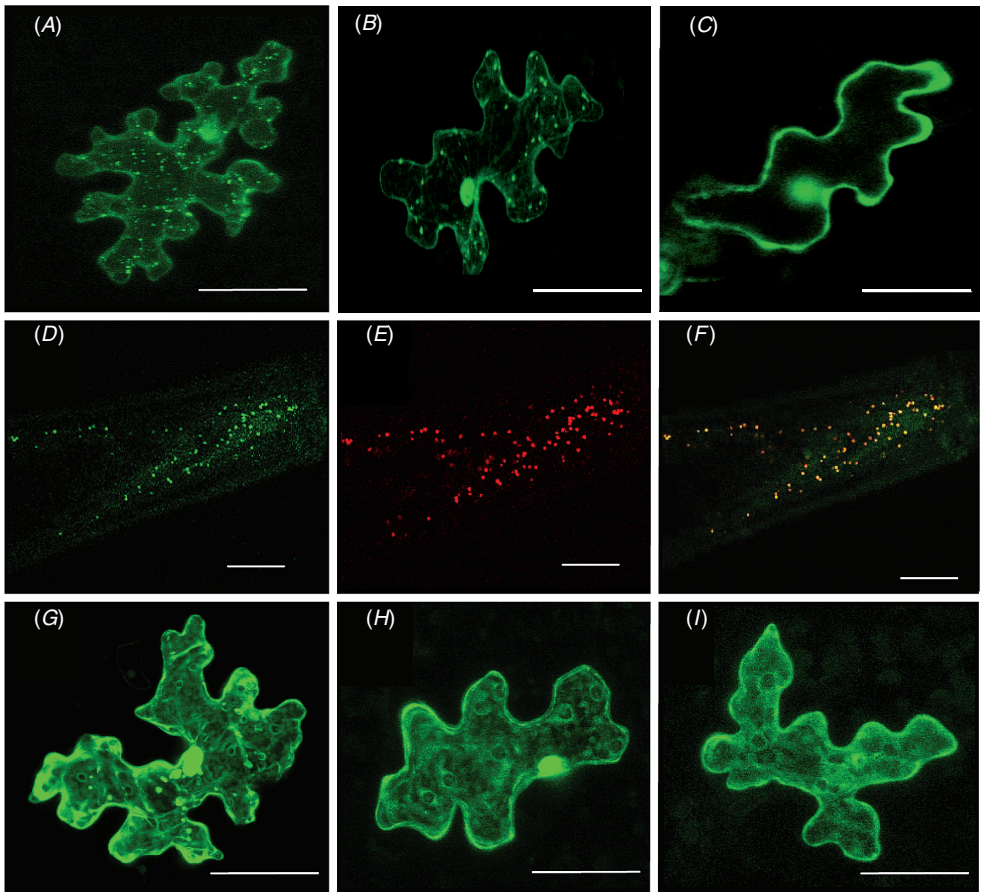

Fig. 4. Subcellular localisation of GFP-AACT1 and GFP-AACT2. Leaves of 15-day-old plants of *Arabidopsis thaliana* L. ecotype Columbia-3 were micro-bombarded with different constructs to express (*A*) GFP-AACT1, (*B*) GFP-SAL, or (*C*) GFP-SALmut. *Allium cepa* L. epidermal cells were microbombarded with constructs to co-express GFP-AACT1 and a monomeric RFP derivative containing the peroxisomal targeting sequence SKL at the C-terminus (Hemmerlin *et al.* 2006): (*D*) green fluorescence, (*E*) red fluorescence and (*F*) merged images. Leaves of 15-day-old plants of *A. thaliana* L. ecotype Columbia-3 were micro-bombarded with (*G*) control non-fused GFP, (*H*) GFP-AACT2 and (*I*) GFP-AACT2-NLSmut. Scale bars correspond to 40 μm.

branching point of axillary inflorescences. The highest level of GUS staining was detected in flowers from early stages of development (Fig. 5*D*). GUS activity in mature flowers was observed in all organs of the four whorls (Fig. 5*E*). After fertilisation and fruit development, GUS activity was restricted to the basal and distal ends of mature siliques (Fig. 5*F*). The GUS expression pattern of the transgenic plants is consistent with the distribution of the *ACT2* transcripts observed by northern blot analysis. To delimit the promoter region of the *ACT2* gene, two 5′-deleted derivatives extending from nucleotides −356 to +291 (construct [−356/+291]*ACT2*::*GUS*) and −121 to +291 (construct [−121/+291]*ACT2*::*GUS*) were generated and stably introduced into *Arabidopsis* by *Agrobacterium*-mediated transformation. The GUS expression pattern observed in the transgenic plants harbouring construct [−356/+291]*ACT2*::*GUS* was equivalent to that described above for construct [−906/+291]*ACT2*::*GUS*. However, the intensity of GUS staining in the [−121/+291]*ACT2*::*GUS* transgenic plants was drastically reduced (data not shown). These results show that the region comprised between nucleotides −356 to −121 contains *cis*-elements that are required for high level expression of the *ACT2* gene.

It is worth noting that the expression patterns reported here for *ACT1* and *ACT2* are in close agreement with the expression data available at the *Arabidopsis* eFP Browser database (http://www.bar.utoronto.ca/efp, accessed 10 January 2008). Interestingly, *ACT1* (but not *ACT2*) is also reported to be highly expressed in seeds.

Discussion

In plants, thiolases participate in essential degradative and biosynthetic processes. In peroxisomes and glyoxysomes of oilseed plants, OACTs are known to play a key role in the β-oxidation of fatty acids during lipid mobilisation after seed germination (Graham and Eastmond 2002). OACT activity has also been proposed to catalyse the three cycles of β-oxidation required for jasmonic acid biosynthesis as well as other β-oxidation processes associated to plant senescence (i.e. the catabolism of branched amino acids) (Graham and Eastmond

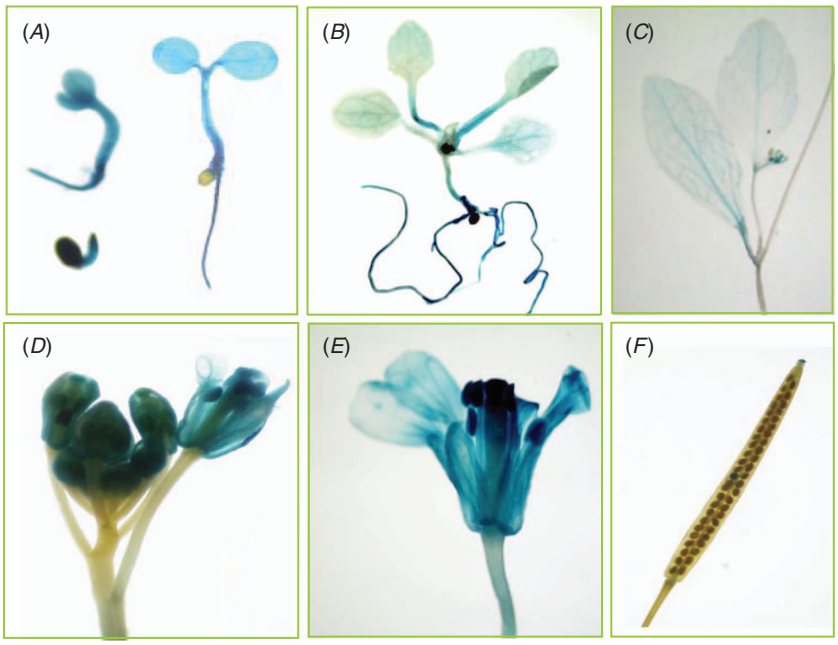

Fig. 5. Histochemical analysis of GUS activity in transgenic *Arabidopsis thaliana* (L.) ecotype Columbia-3 plants. Transgenic plants carrying construct [–906/+291]*ACT2*::*GUS*: germinated seed, (*A*) 2-day-old and 6-day-old seedlings, (*B*) 12-day-old seedling with the first pair of true leaves, (*C*) cauline leaves of an adult plant, (*D*) inflorescence, (*E*) mature flower and (*F*) mature silique.

2002). In the cytosol, AACT plays a role in the MVA pathway by channelling cytosolic acetyl-CoA to the synthesis of isoprenoids (Vollack and Bach 1996; Bach *et al.* 1999).

Five genes encoding thiolases have been annotated in the *Arabidopsis* genome: *At2g33150*, *At1g04710*, *At5g48880*, *At5g48230* and *At5g47720* (http://www.tigr.org). *At2g33150*, *At1g04710*, *At5g48880* correspond to the previously characterised *PED1*/*KAT2*, *KAT1* and *KAT5*/*PKT1–2* genes, respectively, encoding peroxisomal OACTs related with lipid mobilisation after seed germination (Hayashi *et al.* 1998; Germain *et al.* 2001; Graham and Eastmond 2002) and the synthesis of jasmonic acid during leaf senescence and in response to wounding (He *et al.* 2002; Castillo *et al.* 2004). *At5g48880* seems to be a bifunctional gene encoding two OACTs (PKT1 and PKT2), of which only PKT1 contains a N-terminal peroxisomal targeting sequence (Graham and Eastmond 2002). This report describes the characterisation of the *ACT1* (*At5g47720*) and *ACT2* (*At5g48230*) genes which encode functional AACT isoforms (AACT1 and AACT2, respectively). According to the metabolic requirements currently known in plants, it seems reasonable to assume that at least one of the cloned enzymes, most likely AACT2 (see below), participates in the synthesis of isoprenoids through the MVA pathway (Bach *et al.* 1999).

Phylogenetic analyses have shown that AACT1 and AACT2 cluster with cytosolic AACTs from *Saccharomyces cerevisae*, *Saccharomyces uvarum*, *Candida tropicalis* and radish and mitochondrial AACTs from humans and rat. Genetic and biochemical evidence has been provided demonstrating that the AACTs from the above-mentioned yeast species catalyse the first step of the MVA pathway. It has been shown, in addition, that the cDNA encoding radish AACT functionally complements the *erg10* mutant (Hiser *et al.* 1994) from *S. cerevisae* defective in cytosolic AACT (Vollack and Bach 1996). Although human and rat mitochondrial AACTs were originally proposed to be involved in mitochondrial ketone body metabolism, a recent report has shown that these proteins are also targeted to peroxisomes, which are considered as a major site for cholesterol biosynthesis in mammalian cells (Olivier and Krisans 2000; Olivier *et al.* 2000).

The subcellular localisation of AACT1 and AACT2 was analysed by transient expression of chimeric constructs encoding AACT1 and AACT2 fused to the green fluorescent protein GFP. The GFP-AACT2 chimeric protein accumulated in the cytosol, in agreement with the proposed role of AACT2 in the MVA pathway. Unexpectedly, the GFP-AACT2 fusions were also detected in the nucleus. It was found that the amino acid sequence Lys-Lys-Arg located between positions 377 and 379 of AACT2 is required for the transport of the protein to the nuclear compartment. Like in other organisms, the nucleo-cytoplasmic partitioning of proteins is well documented in plants. Although most studies of nucleo-cytoplasmic partitioning in plants have focussed on proteins related with environmental and developmental signalling (Merkle 2003; Silva-Filho 2003) there are examples of enzymes involved in primary metabolism in yeast and animals. For instance glycogen synthase, glucokinase and glyceraldehyde 3-phosphate dehydrogenase are examples of enzymes that accomplish their metabolic function in the cytosol but are also found in the nucleus (Singh and Green 1993; Ferrer *et al.* 1997; De la Iglesia *et al.* 1999). Muscle glycogen synthase and glucokinase were shown to accumulate in the nucleus in the presence of low levels of glucose

and to translocate to the cytosol when the concentration of this sugar increased (Ferrer *et al.* 1997; De la Iglesia *et al.* 1999). Interestingly, it has recently been reported that *Arabidopsis* hexokinase-1, a glycolytic enzyme found in the cytosol, is also present in the nucleus where it participates in a protein complex controlling diverse glucose signalling responses (Cho *et al.* 2006). Thus, it is tempting to speculate that shuttling of AACT2 between the cytosol and the nucleus might contribute to a rapid control of enzyme activity in the cytosol. However, the participation of AACT2 in an as yet unidentified metabolic or signalling process cannot be ruled out.

The GFP-AACT1 fusion protein was localised in peroxisomes. Although unexpected, the localisation of AACT in peroxisomes is not unprecedented. In mammalian cells, AACT activity is found in peroxisomes in addition to the cytosol (Antonenkov *et al.* 2000; Olivier *et al.* 2000). Since mammalian peroxisomes seemingly contain other early enzymes of the MVA pathway, it is assumed that this organelle plays an essential role in cholesterol biosynthesis (Olivier and Krisans 2000). In the yeast *C. tropicalis*, AACT activity has also been detected in peroxisomes in addition to the cytosol. Whereas cytosolic AACT activity was indispensable for the MVA pathway, it has been proposed that peroxisomal AACT cooperates with OACT in the β-oxidation of fatty acids (Kanayama *et al.* 1998). Recently, AACT has been detected and partially purified from sunflower glyoxysomal fractions (Oeljeklaus *et al.* 2002). Although AACT represented a minor fraction of total glyoxysomal thiolytic activity, it has been suggested that this AACT activity could be involved in the degradation of the acetoacetyl-CoA produced during glyoxysomal β-oxidation (Oeljeklaus *et al.* 2002). Since no other enzymes of the MVA pathway have been reported in plant peroxisomes, it seems unlikely that the *Arabidopsis* AACT1 could be involved in isoprenoid biosynthesis.

Peroxisomal proteins are synthesised in the cytosol and targeted to peroxisomes by specific peroxisomal targeting sequences (PTS). Two types of PTS signals have been identified: PTS1, which are located at the C-terminal end of the protein and consist in a non-cleaved tri-peptide motif, and PTS2, which are found at the N-terminal end of the protein and that are removed during translocation (Reumann 2004). In contrast to all plant peroxisomal thiolases identified so far, which possess PTS2 signals (Schiedel *et al.* 2004), the targeting of AACT1 to the peroxisomes relies on a PTS1 motif. Although the C-terminal tri-peptide (Ser-Ala-Leu) found in AACT1 resembles those present in other PTS1 motives, this particular sequence has never been reported in peroxisomal proteins (Hayashi *et al.* 1997; Reumann 2004; Reumann *et al.* 2007). Thus, the C-terminal tri-peptide Ser-Ala-Leu represents a novel PTS1 variant, at least in plants. This observation could be of interest to extend the inventory of potential peroxisomal proteins predicted from plant genomes and other sequence data (Reumann 2004).

In a recent report it was also shown that *Arabidopsis* AACT1 is localised in peroxisomes (Carrie *et al.* 2007). However, the peroxisomal targeting of AACT1 reported by Carrie *et al.* (2007) was associated to an N-terminal extension (PTS2) present in a splicing variant of the protein derived from a transcript not detected in our 5′-RACE experiments. Interestingly, the splicing variant containing the N-terminal extension was lacking the C-terminal extension, thus indicating that the peroxisomal targeting of AACT1 involves two alternative targeting signals (PTS1 and PTS2) resulting from the differential splicing of the *ACT1* primary transcript. The biological significance of the occurrence of two alternative peroxisomal targeting sequences in AACT1 is currently unknown. Recent data derived from the proteomic analysis of *Arabidopsis* leaf peroxisomes has revealed the presence of AACT2 in this organelle (Reumann *et al.* 2007). This finding is difficult to explain according to the current data and may probably reflect cytosolic contamination or a miss-annotation derived from the high similarity between AACT1 and AACT2 proteins. However, the occurrence of an as yet unidentified splicing variant of AACT2 targeted to the peroxisomes cannot be excluded.

The *Arabidopsis ACT2* gene is widely expressed in the plant and its pattern of expression clearly parallels that of other genes of the MVA pathway. As shown here for the *ACT2* gene, the transcripts of *Arabidopsis* genes encoding HMG-CoA reductase (*HMG1*), MVA kinase (*MVK*), farnesyl diphosphate synthase (*FPS1*) and squalene synthase (*SQS1*) accumulate at high levels in seedlings, roots and inflorescences and at lower levels in stems and leaves (Enjuto *et al.* 1994; Cunillera *et al.* 1996; Kribii *et al.* 1997; Lluch *et al.* 2000). In contrast, *ACT1* is expressed at low levels and its expression does not correlate with the expression profile of isoprenoid biosynthetic genes.

Although additional work is still needed to unequivocally assign the metabolic role(s) of AACT1 and AACT2, recent results derived from the characterisation of *Arabidopsis* knockout mutants defective in the *ACT1* or *ACT2* genes (Jin and Nikolau 2007) may give some clues on this respect. Considering that the MVA pathway provides the precursors for the synthesis of a variety of essential plant isoprenoid compounds (e.g. sterols, brassinosteroids, cytokinins and the side chain of ubiquinone), its operation is known to be vital for plant growth ad development (Chappell 1995; Croteau *et al.* 2000; Bouvier *et al.* 2005). In agreement with this, T-DNA insertion mutants affecting the expression of the *ACT2* gene are embryo lethal (Jin and Nikolau 2007). In contrast, null alleles of *ACT1* are viable and have no apparent growth phenotypes (Jin and Nikolau 2007), thus revealing a non-essential role for AACT1. Taken together these results strongly support the involvement of AACT2 in catalysing the first step of the MVA pathway. Although the metabolic role of AACT1 is not clear at present, its peroxisomal localisation, together with the restricted pattern of expression of the *ACT1* gene, suggest a cooperation with peroxisomal OACTs in fatty acid degradation in some particular tissues.

Acknowledgements

This work was supported by grants from the Spanish Ministerio de Educación y Ciencia (BIO2006–03704 to A.B., BFU2006–14655 to N.C. and BIO2005–00367 to M.R.C., all including FEDER funds), and the Generalitat de Catalunya (grant 2005SGR-00914). This work has been carried out within the Centre CONSOLIDER on Agrigenomics funded by the Spanish Ministry of Education and Science. I.A. was recipient of a pre-doctoral MUTIS fellowship from the Agencia Española de Cooperación International. We

thank Aurora Piñas and Antonio Comaposada for their contribution to the isolation and preliminary characterisation of *ACT2* cDNA. We also thank Dr Julio Rozas for his advice in the phylogenetic analysis of thiolases and the staff from the Serveis de Camps Experimentals and Serveis Cientificotecnics of the Universitat de Barcelona for their help in plant culture, DNA-sequencing and confocal laser scanning microscopy.

References

An G (1986) Development of plant promoter expression vectors and their use for analysis of differential activity of nopaline synthase promoter in transformed tobacco cells. *Plant Physiology* **81**, 86–91.

Antonenkov VD, Croes K, Waelkens E, Van Veldhoven PP, Mannaerts GP (2000) Identification, purification and characterization of an acetoacetyl-CoA thiolase from rat liver peroxisomes. *European Journal of Biochemistry* **267**, 2981–2990. doi: 10.1046/j.1432-1033.2000.01314.x

Bach TJ, Boronat A, Campos N, Ferrer A, Vollack KU (1999) Mevalonate biosynthesis in plants. *Critical Reviews in Biochemistry and Molecular Biology* **34**, 107–122. doi: 10.1080/10409239991209237

Bechtold N, Ellis J, Pelletier G (1993) *In planta Agrobacterium* mediated gene transfer by infiltration of adult *Arabidopsis thaliana* plants. *Comptes Rendus de l'Académie des Sciences. Série 3. Sciences de la Vie* **316**, 1194–1199.

Bojorquez G, Gómez-Lim MA (1995) Peroxisomal thiolase mRNA is induced during mango fruit ripening. *Plant Molecular Biology* **28**, 811–820. doi: 10.1007/BF00042067

Bouvier F, Rahier A, Camara B (2005) Biogenesis, molecular regulation and function of plant isoprenoids. *Progress in Lipid Research* **44**, 357–429. doi: 10.1016/j.plipres.2005.09.003

Carrie C, Murcha MW, Millar AH, Smith SM, Whelan J (2007) Nine 3-ketoacyl-CoA thiolases (KATs) and acetoacetyl-CoA thiolases (ACATs) encoded by five genes in *Arabidopsis thaliana* are targeted either to peroxisomes or cytosol but not to mitochondria. *Plant Molecular Biology* **63**, 97–108. doi: 10.1007/s11103-006-9075-1

Castillo MC, Martínez C, Buchala A, Métraux JP, Léon J (2004) Gene-specific involvement of β-oxidation in wound-activated responses in Arabidopsis. *Plant Physiology* **135**, 85–94. doi: 10.1104/pp.104.039925

Chappell J (1995) Biochemistry and molecular biology of the isoprenoid biosynthetic pathway in plants. *Annual Review of Plant Physiology and Plant Molecular Biology* **46**, 521–547. doi: 10.1146/annurev.pp.46.060195.002513

Cho YH, Yoo SD, Sheen J (2006) Regulatory functions of nuclear hexokinase1 complex in glucose signaling. *Cell* **127**, 579–589. doi: 10.1016/j.cell.2006.09.028

Clinkenbeard KD, Sugiyama T, Moss J, Reed WD, Lane MD (1973) Molecular and catalytic properties of cytosolic acetoacetyl coenzyme A thiolase from avian liver. *Journal of Biological Chemistry* **248**, 2275–2284.

Croteau R, Kutchan T, Lewis N (2000) Natural products (secondary metabolites). In 'Biochemistry and Molecular Biology of Plants.' (Eds B Buchanan, W Gruissem, R Jones) pp. 1250–1268. (American Society of Plant Biologists: Rockville, MD)

Cunillera N, Arró M, Delourme D, Karst F, Boronat A, Ferrer A (1996) *Arabidopsis thaliana* contains two differentially expressed farnesyl-diphosphate synthase genes. *Journal of Biological Chemistry* **271**, 7774–7780. doi: 10.1074/jbc.271.13.7774

De la Iglesia N, Veiga-da-Cunha M, Van Schaftingen E, Guinovart JJ, Ferrer JC (1999) Glucokinase regulatory protein is essential for the proper subcellular localisation of liver glucokinase. *FEBS Letters* **456**, 332–338. doi: 10.1016/S0014-5793(99)00971-0

Dean C, van den Elzen P, Tamaki S, Dunsmuir P, Bedbrook J (1985) Differential expression of eight genes of the petunia ribulose bisphosphate carboxylase small subunit multi-gene family. *The EMBO Journal* **4**, 3055–3061.

Enjuto M, Balcells L, Campos N, Caelles C, Arró M, Boronat A (1994) *Arabidopsis thaliana* contains two differentially expressed 3-hydroxy-3-methylglutaryl-CoA reductase genes, which encode microsomal forms of the enzyme. *Proceedings of the National Academy of Sciences of the United States of America* **91**, 927–931. doi: 10.1073/pnas.91.3.927

Felsenstein J (1985) Confidence limits on phylogenies: an approach using the bootstrap. *Evolution* **39**, 783–791. doi: 10.2307/2408678

Ferrer JC, Baqué S, Guinovart JJ (1997) Muscle glycogen synthase translocates from the cell nucleus to the cytosol in response to glucose. *FEBS Letters* **415**, 249–252. doi: 10.1016/S0014-5793(97)01136-8

Frugoli JA, Zhong HH, Nuccio ML, McCourt P, McPeek MA, Thomas TL, McClung CR (1996) Catalase is encoded by a multigene family in *Arabidopsis thaliana* (L.) Heynh. *Plant Physiology* **112**, 327–336. doi: 10.1104/pp.112.1.327

Germain V, Rylott EL, Larson TR, Sherson SM, Bechtold N, Carde JP, Bryce JH, Graham IA, Smith SM (2001) Requirement for 3-ketoacyl-CoA thiolase-2 in peroxisome development, fatty acid b-oxidation and breakdown of triacylglycerol in lipid bodies of *Arabidopsis* seedlings. *The Plant Journal* **28**, 1–12. doi: 10.1046/j.1365-313X.2001.01095.x

Gilbert HF, Lennox BJ, Mossman CD, Carle WC (1981) The relation of acyl transfer to the overall reaction of thiolase I from porcine heart. *Journal of Biological Chemistry* **256**, 7371–7377.

Graham IA, Eastmond PJ (2002) Pathways of straight and branched chain fatty acid catabolism in higher plants. *Progress in Lipid Research* **41**, 156–181. doi: 10.1016/S0163-7827(01)00022-4

Hayashi M, Aoki M, Kondo M, Nishimura M (1997) Changes in targeting efficiencies of proteins to plant microbodies caused by amino acid substitutions in the carboxy-terminal tripeptide. *Plant & Cell Physiology* **38**, 759–768.

Hayashi M, Toriyama K, Kondo M, Nishimura M (1998) 2,4-Dichlorophenoxybutyric acid-resistant mutants of Arabidopsis have defects in glyoxysomal fatty acid b-oxidation. *The Plant Cell* **10**, 183–195. doi: 10.2307/3870697

He Y, Fukushige H, Hildebrand DF, Gan S (2002) Evidence supporting a role of jasmonic acid in Arabidopsis leaf senescence. *Plant Physiology* **128**, 876–884. doi: 10.1104/pp.010843

Hemmerlin A, Reents R, Mutterer J, Feldtrauer JF, Waldmann H, Bach TJ (2006) Monitoring farnesol-induced toxicity in tobacco BY-2 cells with a fluorescent analog. *Archives of Biochemistry and Biophysics* **448**, 93–103. doi: 10.1016/j.abb.2005.10.017

Hiser L, Basson ME, Rine J (1994) *ERG10* from *Saccharomyces cerevisiae* encodes acetoacetyl-CoA thiolase. *Journal of Biological Chemistry* **269**, 31383–31389.

Igual JC, González-Bosch C, Dopazo J, Pérez-Ortín JE (1992) Phylogenetic analysis of the thiolase family. Implications for the evolutionary origin of peroxisomes. *Journal of Molecular Evolution* **35**, 147–155. doi: 10.1007/BF00183226

Jefferson RA (1987) Assaying chimeric genes in plants: the GUS gene fusion system. *Plant Molecular Biology Reporter* **5**, 387–405. doi: 10.1007/BF02667740

Jin H, Nikolau BJ (2007) Genetic, biochemical and physiological studies of acetyl-CoA metabolism via condesation. In 'Current Advances in the Biochemistry and Cell Biology of Plant Lipids.' (Eds C Benning, J Ohlrogge) pp. 177. (Aardvark Global Publishing Company: Salt Lake City, UT)

Kanayama N, Ueda M, Atomi H, Tanaka A (1998) Genetic evaluation of physiological functions of thiolase isozymes in the *n*-alkane-assimilating yeast *Candida tropicalis*. *Journal of Bacteriology* **180**, 690–698.

Kato A, Hayashi M, Takeuchi Y, Nishimura M (1996) cDNA cloning and expression of a gene for 3-ketoacyl-CoA thiolase in pumpkin cotyledons. *Plant Molecular Biology* **31**, 843–852. doi: 10.1007/BF00019471

Köhler RH (1998) GFP for *in vivo* imaging of subcellular structures in plant cells. *Trends in Plant Science* **3**, 317–320. doi: 10.1016/S1360-1385(98)01276-X

Kribii R, Arró M, Del Arco A, González V, Balcells L, Delourme D, Ferrer A, Karst F, Boronat A (1997) Cloning and characterization of the *Arabidopsis thaliana SQS1* gene encoding squalene synthase. Involvement of the C-terminal region of the enzyme in the channeling of squalene through the sterol pathway. *European Journal of Biochemistry* **249**, 61–69. doi: 10.1111/j.1432-1033.1997.00061.x

Kunau WH, Dommes V, Schulz H (1995) b-oxidation of fatty acids in mitochondria, peroxisomes, and bacteria: a century of continued progress. *Progress in Lipid Research* **34**, 267–342. doi: 10.1016/0163-7827(95)00011-9

Lange BM, Ghassemian M (2003) Genome organization in *Arabidopsis thaliana*: a survey for genes involved in isoprenoid and chlorophyll metabolism. *Plant Molecular Biology* **51**, 925–948. doi: 10.1023/A:1023005504702

Lluch MA, Masferrer A, Arró M, Boronat A, Ferrer A (2000) Molecular cloning and expression analysis of the mevalonate kinase gene from *Arabidopsis thaliana. Plant Molecular Biology* **42**, 365–376. doi: 10.1023/A:1006325630792

Madison LL, Huisman GW (1999) Metabolic engineering of poly(3-hydroxyalkanoates): from DNA to plastic. *Microbiology and Molecular Biology Reviews* **63**, 21–53.

Mathieu M, Modis Y, Zeelen JP, Engel CK, Abagyan RA, Ahlberg A, Rasmussen B, Lamzin VS, Kunau WH, Wierenga RK (1997) The 1.8 Å crystal structure of the dimeric peroxisomal 3-ketoacyl-CoA thiolase of *Saccharomyces cerevisiae*: implications for substrate binding and reaction mechanism. *Journal of Molecular Biology* **273**, 714–728. doi: 10.1006/jmbi.1997.1331

Merkle T (2003) Nucleo-cytoplasmic partitioning of proteins in plants: implications for the regulation of environmental and developmental signalling. *Current Genetics* **44**, 231–260. doi: 10.1007/s00294-003-0444-x

Modis Y, Wierenga RK (2000) Crystallographic analysis of the reaction pathway of *Zoogloea ramigera* biosynthetic thiolase. *Journal of Molecular Biology* **297**, 1171–1182. doi: 10.1006/jmbi.2000.3638

Oeljeklaus S, Fischer K, Gerhardt B (2002) Glyoxysomal acetoacetyl-CoA thiolase and 3-oxoacyl-CoA thiolase from sunflower cotyledons. *Planta* **214**, 597–607. doi: 10.1007/s004250100645

Olesen C, Thomsen KK, Svendsen I, Brandt A (1997) The glyoxysomal 3-ketoacyl-CoA thiolase precursor from *Brassica napus* has enzymatic activity when synthesized in *Escherichia coli. FEBS Letters* **412**, 138–140. doi: 10.1016/S0014-5793(97)00766-7

Olivier LM, Krisans SK (2000) Peroxisomal protein targeting and identification of peroxisomal targeting signals in cholesterol biosynthetic enzymes. *Biochimica et Biophysica Acta* **1529**, 89–102.

Olivier LM, Kovacs W, Masuda K, Keller GA, Krisans SK (2000) Identification of peroxisomal targeting signals in cholesterol biosynthetic enzymes. AA-CoA thiolase, HMG-CoA synthase, MPPD, and FPP synthase. *Journal of Lipid Research* **41**, 1921–1935.

Peretó J, Lopez-Garcia P, Moreira D (2005) Phylogenetic analysis of eukaryotic thiolases suggests multiple proteobacterial origins. *Journal of Molecular Evolution* **61**, 65–74. doi: 10.1007/s00239-004-0280-8

Raikhel N (1992) Nuclear targeting in plants. *Plant Physiology* **100**, 1627–1632.

Reumann S (2004) Specification of the peroxisome targeting signals type 1 and type 2 of plant peroxisomes by bioinformatics analyses. *Plant Physiology* **135**, 783–800. doi: 10.1104/pp.103.035584

Reumann S, Babujee L, Ma C, Wienkoop S, Siemsen T *et al*. (2007) Proteome analysis of *Arabidopsis* leaf peroxisomes reveals novel targeting peptides, metabolic pathways, and defense mechanisms. *The Plant Cell* **19**, 3170–3193. doi: 10.1105/tpc.107.050989

Rodríguez-Concepción M, Yalovsky S, Zik M, Fromm H, Gruissem W (1999) The prenylation status of a novel plant calmodulin directs plasma membrane or nuclear localization of the protein. *The EMBO Journal* **18**, 1996–2007. doi: 10.1093/emboj/18.7.1996

Schiedel AC, Oeljeklaus S, Minihan P, Dyer JH (2004) Cloning, expression, and purification of glyoxysomal 3-oxoacyl-CoA thiolase from sunflower cotyledons. *Protein Expression and Purification* **33**, 25–33. doi: 10.1016/j.pep.2003.08.022

Silva-Filho MC (2003) One ticket for multiple destinations: dual targeting of proteins to distinct subcellular locations. *Current Opinion in Plant Biology* **6**, 589–595. doi: 10.1016/j.pbi.2003.09.008

Singh R, Green MR (1993) Sequence-specific binding of transfer RNA by glyceraldehyde-3-phosphate dehydrogenase. *Science* **259**, 365–368. doi: 10.1126/science.8420004

Vollack KU, Bach TJ (1996) Cloning of a cDNA encoding cytosolic acetoacetyl-Coenzyme A thiolase from radish by functional expression in *Saccharomyces cerevisiae. Plant Physiology* **111**, 1097–1107. doi: 10.1104/pp.111.4.1097

Wille A, Zimmermann P, Vranová E, Fürholz A, Laule O *et al*. (2004) Sparse graphical Gaussian modeling of the isoprenoid gene network in *Arabidopsis thaliana. Genome Biology* **5**, R92. doi: 10.1186/gb-2004-5-11-r92

Zhong HH, Young JC, Pease EA, Hangarter RP, McClung CR (1994) Interactions between light and the circadian clock in the regulation of CAT2 expression in Arabidopsis. *Plant Physiology* **104**, 889–898.